LPSC 09-167
LYCEN 2009-12

Dileptonic signatures of T-odd quarks at the LHC

Giacomo Cacciapaglia[1*], S. Rai Choudhury[2†], Aldo Deandrea[1‡], Naveen Gaur[3§], Michael Klasen[4¶]

[1] *Université de Lyon, F-69622 Lyon, France; Université Lyon 1, CNRS/IN2P3, UMR5822 IPNL, F-69622 Villeurbanne Cedex, France*
[2] *Center for Theoretical Physics (CTP), Jamia Millia University, Delhi & Indian Institute of Science Education & Research (IISER), Govindpura, Bhopal, India*
[3] *Department of Physics & Astrophysics, University of Delhi, Delhi - 110007, India*
[4] *Laboratoire de Physique Subatomique et de Cosmologie, Université Joseph Fourier/CNRS-IN2P3/INPG, 53 Avenue des Martyrs, 38026 Grenoble, France*

Abstract

Little Higgs models are often endowed with a T-parity in order to satisfy electroweak precision tests and give at the same time a stable particle which is a candidate for cold dark matter. This type of models predicts a set of new T-odd fermions in addition to the heavy gauge bosons of the Little Higgs models, which may show interesting signatures at colliders. In this paper, we study the signatures of strong and electroweak pair production of the first two generations of T-odd quarks at the LHC. We focus on the dileptonic signatures (a) $pp \to \ell^\pm \ell^\mp jj \not{E}_T$ (opposite-sign dileptons) and (b) $pp \to \ell^\pm \ell^\pm jj \not{E}_T$ (same-sign dileptons).

*g.cacciapagalia@ipnl.in2p3.fr
†srai.choudhury@gmail.com
‡deandrea@ipnl.in2p3.fr
§gaur.nav@gmail.com
¶klasen@lpsc.in2p3.fr

I Introduction

One of the problems affecting the Standard Model (SM) of particle physics is the hierarchy between the electroweak scale and the Planck scale. Within the SM, the Higgs boson receives a quadratically divergent contribution to its mass, if the model is considered an effective theory, valid only up to some high energy scale. However, precision electroweak measurements at colliders and at low energy clearly show that the physics behind the SM is perturbative in nature. This means that the Higgs boson mass cannot be very large and that the scale of new physics affecting those observables is larger than about 10 TeV, thus requiring fine-tuning between this new scale and the electroweak scale [1]. In Little Higgs models (see [2] for two recent reviews), the Higgs field is a Nambu-Goldstone boson (NGB) of a global symmetry, which is spontaneously broken at some higher scale f by a vacuum expectation value. The Higgs field gets a mass through symmetry breaking at the electroweak scale. However, since it is protected by the approximate global symmetry, it remains light. Generic Little Higgs models predict, at a scale of the order of f, new particles responsible for canceling the SM quadratic divergences at the one-loop level: heavy $SU(2)\times U(1)$ gauge bosons, new heavy scalars and new fermions, in particular partners of the top quark. The original Little Higgs models allowed tree-level couplings of the new particles to the SM ones, inducing tree and loop level contributions to various electroweak precision observables. Performing an analysis of the precision data for generic regions of the parameter space, a lower bound on the symmetry breaking scale f of several TeV was derived [3], reintroducing the fine tuning problem between the cut-off scale of the models ($\sim 4\pi f$) and the electroweak scale. This resulted in addition in new Little Higgs particles that were too heavy to be observed at the LHC.

In order to render this kind of models consistent with precision data and to address the fine tuning problem, a new discrete parity named T-parity (similar to R-parity in Supersymmetry) was introduced [4]. This new class of models, known as *Little Higgs models with T-parity (LHT)*, includes new heavy particles, which are postulated to be odd under T-parity. As a consequence, all the T-odd particles can only be produced in pairs, so that they introduce no tree-level contributions to electroweak observables. As the corrections to precision observables now enter only at the loop level, they are naturally small. The introduction of T-parity therefore allows to lower the new particle mass scale to $f \sim 500$ GeV. In order to consistently implement T-parity, one has to introduce sets of T-odd fermions corresponding to each of the SM fermions. All the heavy particles introduced (except for a vector-like heavy top quark T_+) are odd under T-parity. These T-odd fermions have a mass of the order of f and can thus be abundantly produced at future colliders. LHT models also provide a possible candidate for dark matter that is odd under T-parity, namely a heavy photon A_H.

Recently, the proton-proton Large Hadron Collider (LHC) has become operational at CERN. One of the main focuses of this machine is the discovery of the SM Higgs boson. In addition, it can probe various new physics models. In this work we will focus on the possibility of the production of the first two generations of T-odd quarks at the LHC. In particular we will focus on the dileptonic

signatures. The signatures we will study are (a) $pp \to \ell^\pm \ell^\mp jj \not{E}_T$ and (b) $pp \to \ell^\pm \ell^\pm jj \not{E}_T$. The former was also studied in [5], where the authors considered the pair production of T-odd quarks in the channel $pp \to Q_H \bar{Q}_H$. They argued that this production channel was QCD-dominated (with $q\bar{q}$ and gg in the initial state), and they neglected the electroweak (EW) contributions to it. In our study we will show that the EW contributions to these production channels are substantial. As the EW contributions are not negligible, one can also have the T-odd quark pair production via EW processes like $uu \to U_H U_H$ etc., giving a signature of same-sign dileptons in the final state. The same-sign dilepton process has very small SM backgrounds and can therefore be very useful for observing the LHT model at the LHC. In our analysis we have used modified couplings of T-odd fermions, which assure the correct cancellation of ultraviolet divergences in Z-penguin diagrams in various flavour-changing decays [6].

Our paper is organized as follows: In Sec. II, we present the novel aspects of our analysis. In Sec. III, we introduce briefly the particular LHT model that we have considered. In Sec. IV, we discuss the production cross sections and branching fractions of the pair production of the T-odd quarks and their dependence on the LHT model parameters. In Sec. V, we describe our analysis set-up for both signal and background processes. Finally, we conclude with a summary of our results in Sec. VI.

II Overview

The production and signatures of T-odd quarks at the LHC have previously been discussed in Refs. [5, 7, 8]. In our analysis:

- we have included the v^2/f^2 corrections to the SM Z- and W-boson couplings to the mirror fermions as pointed out in Ref. [6][1];
- we have performed a detailed realistic simulation by using the fast detector simulator ATLFAST [9] for both signal and background processes;
- we have considered the electroweak (EW) contributions to the production processes that have been neglected in Ref. [5];
- we have analyzed same-sign dilepton signatures that had not been not considered in Refs. [5, 7, 8]; note that for these signatures the SM backgrounds are very small, so that this mode can be very useful to discover the T-odd quarks at the LHC;
- we have given the K-factors for the production of T-odd quarks via QCD and EW diagrams, and we have included K-factors for both signal and backgrounds in our simulation results.

[1] The revised CALCHEP model files that include the new corrections to the couplings of mirror quarks to Z- and W-bosons can be downloaded from `http://deandrea.home.cern.ch/deandrea/LHTmodl.tgz`.

III The model

As an example for a typical spectrum of new particles introduced in Little Higgs models with T-parity, we consider the Littlest Higgs model with T-parity [10, 11, 12]. We only briefly review here the aspects of the model relevant for our analysis. The model we have considered has a $SU(5)$ global symmetry that is broken down to $SO(5)$. The $[SU(2) \times U(1)]^2$ subgroup of $SU(5)$ is gauged and is broken down to the diagonal subgroup $SU(2)_L \times U(1)_Y$, that is identified with the SM electroweak gauge group. The masses of the heavy T-odd gauge bosons are

$$M_{A_H} \simeq \frac{g' f}{\sqrt{5}}, \quad M_{V_H} \simeq g f, \tag{1}$$

where g' and g denote the hypercharge and $SU(2)$ weak couplings, respectively. A_H is usually the lightest T-odd particle[2].

Concerning the implementation of T-parity in the fermion sector, each SM fermion doublet is replaced by a pair of fields $F_i\,(i = 1, 2)$, where F_i is a doublet under one $SU(2)_i$ and a singlet under the other. T-parity exchanges F_1 and F_2. The T-even combination is identified with the SM fermion doublet, and the other (T-odd) combination is the heavy partner F_H. To generate mass terms for these T-odd heavy fermions through Yukawa interactions, one requires additional T-odd $SU(2)$ singlet fermions in the theory. Assuming for simplicity a universal and flavour diagonal Yukawa coupling κ, we have for the heavy up-quark U_H and the heavy down-quark D_H (the T-odd heavy partners of the SM quarks (u, c) and (d, s), respectively)

$$M_{D_{H,i}} \simeq \sqrt{2}\,\kappa_i\, f\ , \qquad M_{U_{H_i}} \simeq \sqrt{2}\,\kappa_i\, f\,\left(1 - \frac{v_{\rm SM}^2}{8\, f^2}\right)\ . \tag{2}$$

The up- and down-type T-odd heavy quarks have nearly equal masses, as the scale f is typically at least in the 500 GeV range or more. The Yukawa couplings κ_i depend in general on the fermion species i. This can in turn generate Flavour Changing Neutral Current (FCNC) interactions in the quark sector [14]. Similar phenomena can also occur in the lepton sector, giving rise to Lepton Flavour Violation (LFV) in this class of models [6, 15]. For our analysis, we will assume that the κ_i are flavour-blind and universal and hence do not give rise to any new sources of flavour violation. The top sector requires typically an additional T-even fermion T_+ and a T-odd T_- to cancel the Higgs quadratic divergences. The cancellation of the quadratic divergence in the Higgs boson mass is not due to the T-odd states, but it is achieved by loops involving the SM top quark and the heavy T-even top quark. For a different implementation of the heavy top sector in T-parity models see Ref. [16].

The LHT parameters relevant for our analysis are f and κ. In our analysis we will assume that the values of κ are sufficiently smaller than the upper bound obtained from four-fermion operators: $M_{\rm TeV} \leq 4.8 f_{\rm TeV}^2$ [12] where $M_{\rm TeV}$ and $f_{\rm TeV}$ are the T-odd fermion masses and symmetry breaking scale, respectively, in TeV. For our analysis we have chosen three representative points with values of $\kappa = 0.6, 1$ and 1.5.

[2]There is a possibility of the T-odd neutrino to be a dark matter candidate; this has been explored in [13].

IV Production and decays of the first two generations of T-odd quarks at the LHC

We compute the cross sections for the pair production of the first two generations of T-odd quarks at the LHC and their branching fractions based on the model briefly defined in Sec. III and using CalcHEP 2.5.4 [17]. As described earlier, we have modified the LHT model files for CalcHEP as proposed in Ref. [8] to include the new v^2/f^2 contributions to the couplings of mirror fermions to the SM W- and Z-bosons. All the cross sections are calculated for a LHC centre-of-mass energy of 14 TeV. We have used the leading order (LO) CTEQ6L parton densities with two-loop α_s and $\Lambda_{\overline{\rm MS}}^{n_f=5} = 226$ MeV [18] and identified both the factorization scale μ_f and the renormalization scale μ_r with the partonic centre-of-mass energy $\hat{s}$.

A Decays of first- and second-generation T-odd quarks

The T-odd quarks will decay into a T-odd particle and a T-even SM particle. The decay pattern is determined by the mass spectrum of the T-odd particles. In LHT, we have typically

$$m_{A_H} \simeq \frac{g' f}{\sqrt{5}} \simeq 0.156 f \ , \quad m_{V_H} \simeq g f \simeq 0.653 f \ , \quad m_{Q_H} \simeq \sqrt{2}\kappa f \simeq 1.414 \kappa f \ , \tag{3}$$

where m_{V_H} and m_{Q_H} are the T-odd W-boson, Z-boson and quark masses, respectively. We show the branching ratios of the up-type (U_H) and down type (D_H) T-odd quarks as a function of κ in Fig. 1.

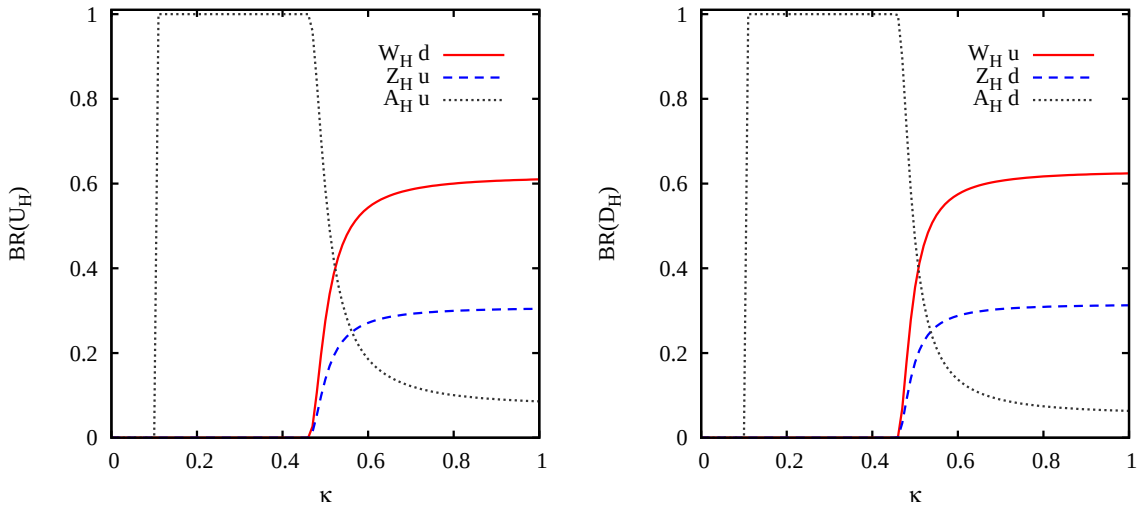

Figure 1: *Branching ratios of T-odd up-type (U_H, left panel) and down-type (D_H, right panel) heavy quarks as a function of κ for a symmetry breaking scale of $f = 1000$ GeV.*

From the spectrum of T-odd particles, we can observe that A_H is always lighter than W_H. When $\kappa < 0.11$, one obtains a mass hierarchy $m_{Q_H} < m_{A_H} < m_{W_H}$. In this case, the T-odd

fermion would be a dark matter candidate, but as discussed in Ref. [19], the dark matter candidate should be a neutral and colourless object. So for our analysis we will work in the parameter space where $\kappa > 0.11$. When $0.11 < \kappa < 0.462$, the mass spectrum is $m_{A_H} < m_{Q_H} < m_{W_H}$. In this case, the dominant decay mode of the T-odd heavy quark is $Q_H \to A_H q$. If $\kappa > 0.462$, we have the mass spectrum $m_{A_H} < m_{W_H} < m_{Q_H}$, and as shown in Fig. 1, the T-odd quark will predominantly decay through the channel $Q_H \to W_H q'$. In our analysis, we will restrict ourselves to the parameter space $\kappa > 0.462$, where $\mathrm{BR}(W_H \to A_H W) = 100\,\%$.

If the masses of the first two generations of T-odd quarks are not too high, they can be produced in large numbers at the LHC. Assuming that the SM W-bosons decay leptonically, the T-odd quarks for $\kappa > 0.46$ predominately follow the decay chains

$$\begin{aligned}
U_H &\to W_H^+ d \to W^+ A_H d \to \ell^+ \nu A_H d \to \ell^+ j \not{E}_T, \\
D_H &\to W_H^- u \to W^- A_H u \to \ell^- \bar{\nu} A_H u \to \ell^- j \not{E}_T, \\
\bar{U}_H &\to W_H^- \bar{d} \to W^- A_H \bar{d} \to \ell^- \bar{\nu} A_H \bar{d} \to \ell^- j \not{E}_T, \\
\bar{D}_H &\to W_H^+ \bar{u} \to W^+ A_H \bar{u} \to \ell^+ \nu A_H \bar{u} \to \ell^+ j \not{E}_T,
\end{aligned} \tag{4}$$

whose probability is approximately 12% (taking into account the branching ratio of the U_H and D_H decays, and the leptonic decay of the W, where the lepton is either an electron or a muon). In our analysis we will focus on the decay chains of T-odd heavy quarks as listed above.

B Production cross sections at the LHC

The pair production of T-odd quarks at the LHC has been considered in Refs. [5, 7, 8]. A detailed signal and background estimation of the pair production of T-odd quarks was carried out by Choudhury *et al.* [5] using a parton-level Monte Carlo generator, where the authors considered in particular the $\ell^\pm \ell^\mp jj \not{E}_T$ signature. This signature is generated by the following production channels:

$$pp \to Q_H \bar{Q}_H, \qquad \text{with} \quad Q_H = U_H, D_H, C_H, S_H \quad (\mathrm{QCD} + \mathrm{EW}), \tag{5}$$

$$pp \to Q_H Q'_H + c.c., \quad \text{with} \quad Q_H = U_H, C_H, \quad Q'_H = D_H, S_H \quad (\mathrm{EW}). \tag{6}$$

Choudhury *et al.* considered only the QCD part of the production channels given in Eq. (5), arguing that the EW amplitudes would be much smaller than those mediated by QCD. We have evaluated the production cross sections of both channels given in Eqs. (5) and (6). Our results are shown in Fig. 2. For comparison with the results in literature, we have chosen the same set of input parameters as in Fig. 1 of Choudhury *et al.* [5]. As it can be seen from our figure, the EW contribution can substantially alter the QCD results, and in some cases the full cross section is enhanced by one order of magnitude.

The reason why the EW contribution is in this case substantial is the following: the EW contributions are basically t-channel diagrams with $1/(t - m^2)$ dependence, which leads to large

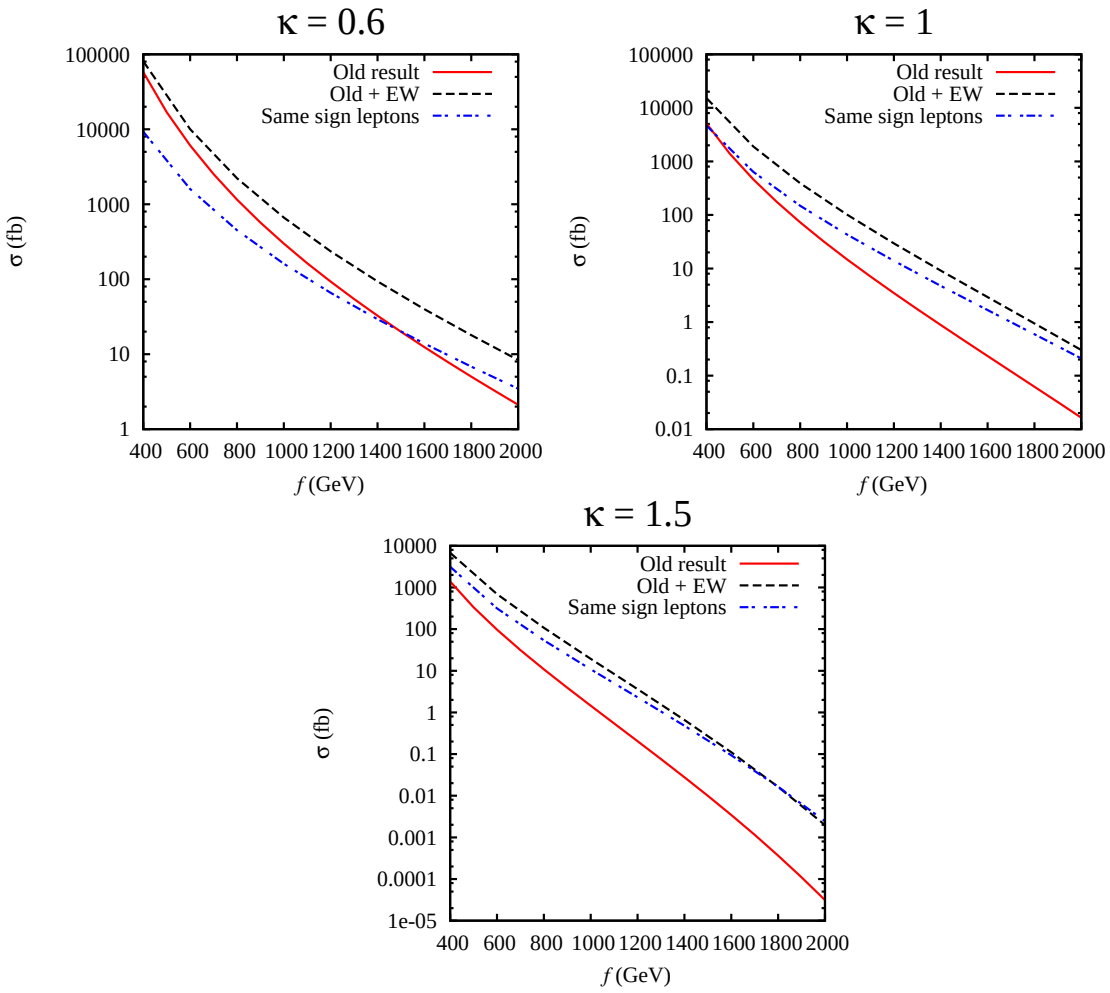

Figure 2: *Production cross sections for a pair of T-odd quarks at the LHC with a centre-of-mass energy of 14 TeV. The plots include all the channels in Eqs. (5) and (6). The label "Old result" corresponds to pure QCD contributions [5], while the label "Old + EW" represents the complete set of QCD + EW diagrams. The label "Same sign leptons" marks the cross sections for the EW channels in Eq. (7), which contribute to the same-sign lepton signature.*

contributions in the near-forward region of $\cos\theta = 1$. Here, t is the invariant momentum transfer squared, m is the mass of the exchanged particle, and θ is the angle between the initial and final state particles in the centre-of-mass frame. This behaviour is very different from the s-channel diagrams, which dominate the QCD contributions and have a regular $(1 + \cos^2\theta)$ dependence. If the particle masses and couplings in a particular model are suitably chosen, then it is indeed possible for s-channel diagrams to fall off more rapidly with $1/s$ than the t-channel diagrams. This is exactly what is happening in the LHT model considered here, despite the suppression due to the weak couplings.

Figure 2 clearly indicates that EW diagrams, via t-channel exchange, can be comparable to

s-channel QCD contributions. It is then interesting to consider purely weak processes like

$$pp \to Q_H \bar{Q}'_H + c.c., \quad \text{with } Q_H = U_H, C_H, \quad Q'_H = D_H, S_H. \tag{7}$$

These channels, following the decay chains in Eqs. (4), give rise to same-sign dilepton signatures, $\ell^\pm\ell^\pm jj \not{E}_T$, with two same-sign leptons, two light jets, and missing transverse energy E_T. Same-sign dileptons have relatively small SM backgrounds and are therefore very distinctive for physics beyond the SM. In Fig. 2, we have also shown the production cross section for the processes given in Eq. (7).

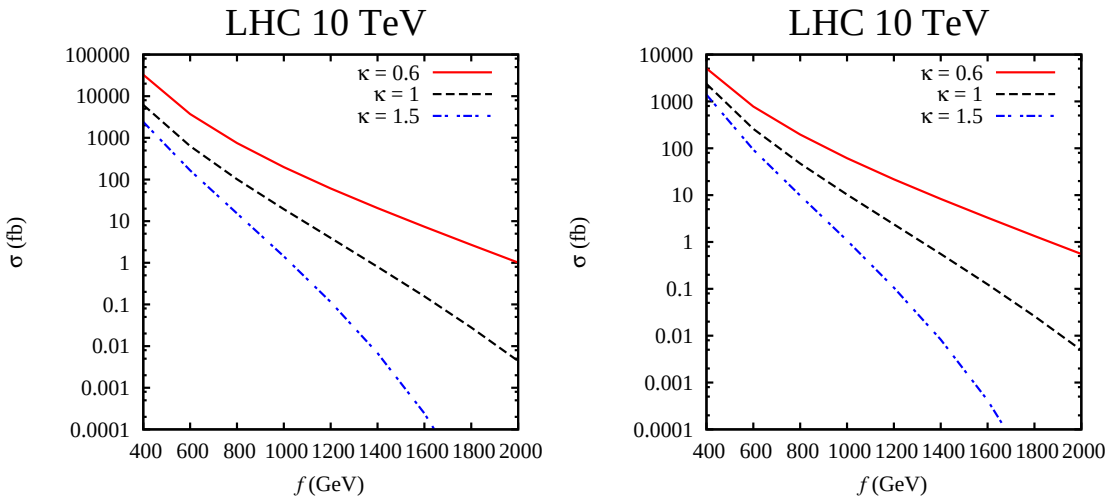

Figure 3: *Production cross sections at the LHC with a centre-of-mass energy of 10 TeV for different-sign dilepton channels (left panel) and same-sign dilepton channels (right panel).*

As can be seen from Fig. 2, the production cross sections for processes giving rise to opposite-sign dileptons ($\ell^\pm\ell^\mp jj \not{E}_T$) could be of the the order of a picobarn, and those contributing to same-sign dileptons ($\ell^\pm\ell^\pm jj \not{E}_T$) could be of the order of few hundred femtobarn for a reasonable range of allowed parameter space in our LHT model. At the moment, the program for the early LHC running consists of a first run for $\sqrt{s} = 7$ TeV at very low luminosity (< 100 pb^{-1}), followed by an upgrade to $\sqrt{s} \sim 10$ TeV with a luminosity of $\mathcal{L} \sim \mathcal{O}(100)$ pb^{-1} [20]. In Fig. 3, we therefore also show the cross sections of the two channels at the LHC with a centre-of-mass energy of 10 TeV. It can be seen that even in very early stages and with a lower energy of 10 TeV it is possible to copiously produce large number of T-odd quarks in a reasonable range of LHT model parameter space. However, for our simulations we will assume an LHC run at 14 TeV. Armed with the production cross sections and decay rates for the signal processes, we will discuss in next section in detail the signal and background event rates.

V Signal and background estimates

In this section we will compute estimates for the signal and backgrounds events. We will also study various kinematical distributions for both signal and backgrounds that can be useful in extracting the signal from the backgrounds. In our analysis, we have chosen three LHT model parameter space points. The mass spectra of LHT particles relevant for our study are given in Tab. 1.

Table 1: *Input parameters and masses of the LHT particles used for our analysis.*

Model parameters → Particle masses (in GeV) ↓	$f = 1000$ GeV $\kappa = 0.6$	$f = 1000$ GeV $\kappa = 1$	$f = 700$ GeV $\kappa = 1.5$
M_{A_H}	150	150	100
M_{V_H}	648	648	450
M_{U_H}	842	1403	1462
M_{D_H}	848	1414	1484

A Framework for event generation

The set-up used for signal and background generation is the following:

- **Signal event generation:** We have used CalcHEP 2.5.4 [17] to calculate cross sections and branching ratios. As described earlier, we have modified the LHT model file given by the authors in Ref. [8]. The original LHT model file for CalcHEP [8] does not have a QNUMBERS block for the new particles, although the new version of CalcHEP (2.5.4) is compatible with this block. Apart from other modifications described earlier, we have also introduced this block and accordingly passed the Monte Carlo numbers to the new set of particles in the revised model files. The parton level events generated by CalcHEP 2.5.4 were then passed on to PYTHIA 6.4.21 [21] via the LHE (Les Houches Event) interface [22] in order to include initial and final state radiation (ISR/FSR) effects.

- **Background event generation:** We have generated the $t\bar{t}$ backgrounds using PYTHIA 6.4.21, still including ISR/FSR effects. The $W^{\pm}W^{\mp}jj$, $W^{\pm}W^{\pm}jj$, $ZZjj$ backgrounds were generated using MADGRAPH [23] and were then passed on to PYTHIA 6.4.21 for ISR/FSR effects.

The K-factors for both signal and background processes have been computed with MCFM 5.6 [24], using for the LO cross sections the same LO parton densities as in the full simulation, i.e. CTEQ6L with two-loop α_s and $\Lambda_{\overline{\rm MS}}^{n_f=5} = 226$ MeV [18]. For the next-to-leading order (NLO) cross sections, we used the most recent NLO parton densities CTEQ6.6M with an improved treatment of heavy-quark effects through a general-mass variable-flavor number scheme [25]. In

Table 2: *Applied K-factors for the QCD and EW contributions to the signal process as a function of the heavy-quark mass m_{Q_H}.*

m_{Q_H}/GeV	200	400	600	800	1000	1200	1400	1600	1800	2000
QCD K-factor	1.20	1.43	1.51	1.54	1.56	1.58	1.58	1.52	1.46	1.42
EW K-factor	1.03	1.17	1.29	1.41	1.53	1.68	1.84	2.01	2.24	2.39

Table 3: *Applied K-factors for the considered background processes.*

Final state	$t\bar{t}$ (QCD)	$t\bar{t}$ (EW)	W^+jj	W^-jj	Zjj
K-factor	1.16	1.01	1.52	1.47	1.32

both cases, we identified the factorization scale μ_f and the renormalization scale μ_r with the partonic centre-of-mass energy $\hat{s}$.

To be specific, the K-factors for the QCD signal cross section were computed from $t\bar{t}$ production by increasing the top-quark mass from 175 GeV to generic heavy-quark mass values of up to 2 TeV (see the second line in Tab. 2). This is possible, since the QCD properties of T-odd quarks are identical to those of the SM heavy quarks. Using the same method and similar parton densities, but setting the scales to the heavy-quark mass, results at NLO+NLL (next-to-leading logarithmic level) have been obtained for the LHC in Tab. 4 of Ref. [26]. Since NLL results are not available for EW production and the background processes and in order to employ the same scales for all signal and background processes, we do not make use of these cross sections here. The NLO+NLL cross sections are moreover considerably higher than ours, so that our estimate of corrected signal cross sections and consequently of the significance is quite conservative.

K-factors for the electroweak signal cross sections cannot be computed with MCFM, since the s-channel single-top production process $q\bar{q}' \to t\bar{b}$ was computed there with $m_b = 0$. Instead, we take them from the t-channel process $qg \to qt'\bar{b}'$ with $m_{b'} = m_{t'}$ as tabulated in Tab. 10 of Ref. [27], averaging over opposite charges of the heavy-quark final state (see the third line in Tab. 2). The QCD and EW K-factors as a function of the heavy-quark mass in Tab. 2 lend themselves to quadratic and linear fits, respectively,

$$K_{\rm QCD} \;=\; 1.58 - \left(\frac{m_{Q_H}/\text{GeV} - 1200}{2000}\right)^2 , \; K_{\rm EW} \;=\; \frac{m_{Q_H}/\text{GeV} + 1200}{1400}, \tag{8}$$

which we have used in our full signal simulation.

The K-factors for the QCD and EW production of the SM $t\bar{t}$ background have been computed for $m_t = 175$ GeV as described above and are tabulated in the second and third columns of Tab. 3. However, the K-factors for the $WW + 2$ jet and $ZZ + 2$ jet backgrounds are not yet available in the literature. We therefore computed with MCFM the $W + 2$ jet and $Z + 2$ jet K-factors

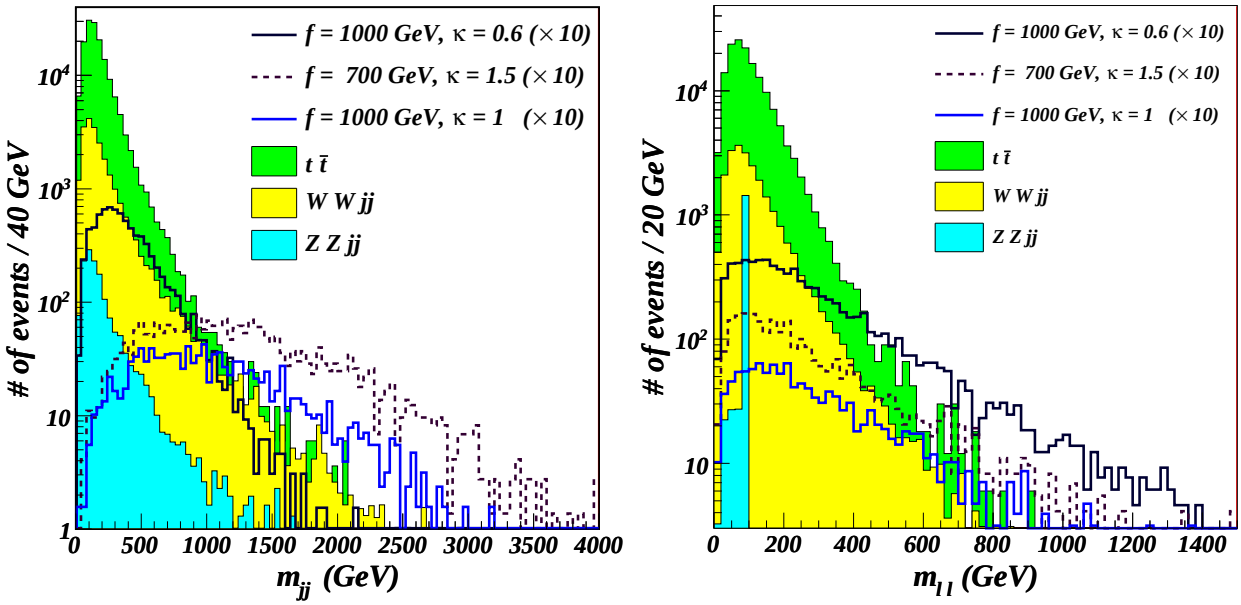

Figure 4: *Dijet invariant mass (m_{jj}) distribution (left panel) and di-lepton invariant mass ($m_{\ell^\pm\ell^\mp}$) distribution (right panel) for signal ($\times 10$) and SM background in the channel $pp \to Q_H Q'_H \to jj\ell^+\ell^- \not{E}_T$. In plotting these distributions we have assumed the LHC luminosity to be $\mathcal{L} = 100$ fb^{-1}.*

and assumed that the second vector boson, being uncharged under color, does not change the K-factors significantly. For these backgrounds, we implemented all the kinematic cuts described below. In particular, the jets were identified with the midpoint cone algorithm of radius $R = 0.7$ and parton separation $R_{\rm sep} = 1.3R$. The $Z + 2$ jet background required in addition a minimum invariant mass cut for the charged-lepton pair, which we have set to 15 GeV as in Ref. [28]. Our results are listed in columns four to six of Tab. 3.

In order to make realistic estimates of the signal and backgrounds, we have further processed both the signal and background events through the fast ATLAS detector simulator ALTFAST [9]. The resulting events have been analysed within the ROOT framework. The detector simulator ATLFAST provides a simple detector simulation and jet reconstruction using a simple cone algorithm. It also identifies isolated leptons, photons, b and τ jets and also reconstructs the missing energy. In our analysis, leptons means electrons or muons *i.e.* $\ell = e, \mu$. As stated above, we have assumed an LHC with a centre-of-mass energy of 14 GeV and luminosity $\mathcal{L} = 100$ fb^{-1}.

B Opposite-sign dilepton signatures: $\ell^\pm\ell^\mp jj \not{E}_T$

This signature is generated by the production processes given in Eqs. (5) and (6) and the decay chains given in Eqs. (4).

The possible SM background sources to this signal are:

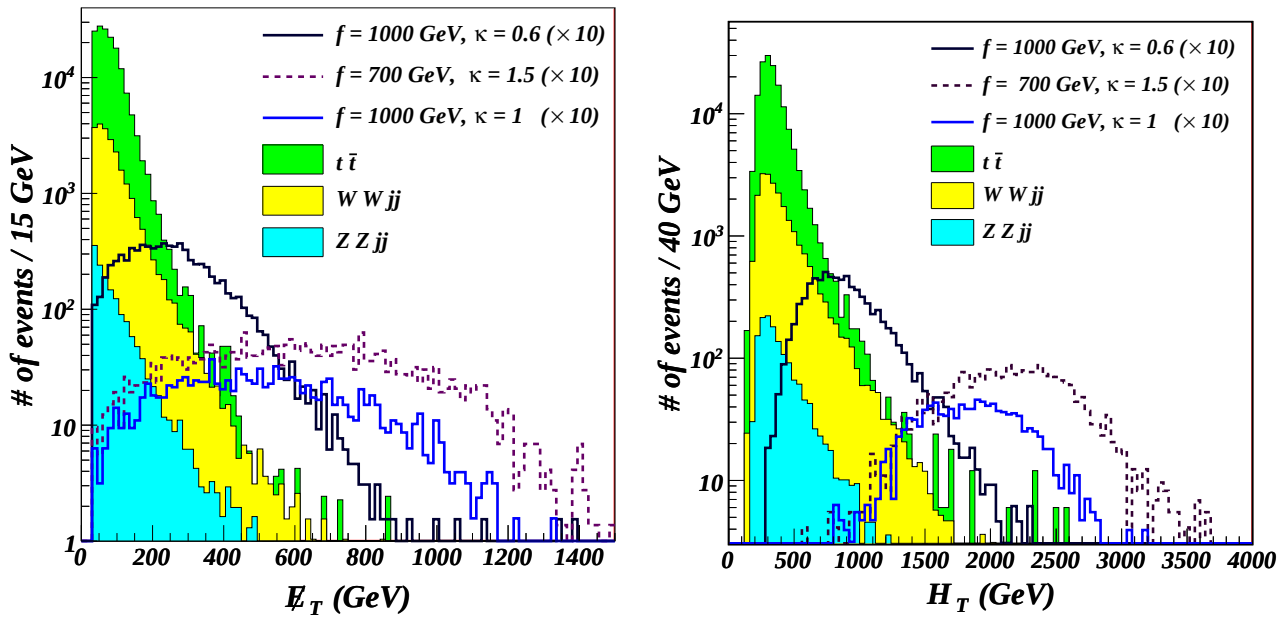

Figure 5: *$\not{E}_T$ and H_T distributions for signal ($\times 10$) and SM background in the channel $pp \to Q_H Q'_H \to jj\ell^+\ell^- \not{E}_T$. In plotting these distributions we have assumed the LHC luminosity to be $\mathcal{L} = 100\ fb^{-1}$.*

- $pp \to t\bar{t}$ with each of the two top quarks decaying via $t \to bW(\to \ell\nu) \to b\ell\ \not{E}_T$ and the b-jet misidentified as a light jet.
- $pp \to W^+W^-jj$ with both W-bosons decaying leptonically through $W \to \ell\nu$.
- $pp \to ZZjj$ with one of the Z-bosons decaying via $Z \to \ell^+\ell^-$ and the other Z-boson decaying to neutrinos $Z \to \nu\bar{\nu}$.

In order to study the signal and background, we have implemented the following *pre-selection* cuts :

(a) exactly two opposite charge leptons (e, μ) in the event with $p_T^\ell > 15$ GeV and rapidity in the range $|\eta| < 2.5$;

(b) b-jet veto (reject any event having a well identified b-jet); we have considered a b-tagging efficiency of 60%; this cut helps in reducing the $t\bar{t}$ background;

(c) exactly two light jets with $p_T^j > 30$ GeV and $|\eta| < 2.5$;

(d) minimum missing energy threshold: $\not{E}_T > 30$ GeV;

(e) minimum threshold for the opposite-sign dilepton invariant mass $m_{\ell^+\ell^-} > 15$ GeV; this helps in reducing the backgrounds where the lepton pair originates from a virtual photon.

We have shown the dijet (for lighter jets) invariant mass distribution (m_{jj}) and the opposite-sign dilepton invariant mass distribution ($m_{\ell\ell}$) for signal and backgrounds in Fig. 4. As it can be observed from these distributions, we can reduce the backgrounds, where the lepton pair and the jet pair originate from a Z- or W-boson. For this we impose the extra condition that the invariant mass of jets and leptons are away from M_Z and M_W, respectively. So we demand:

$$m_{jj} \notin [65, 105]\ GeV\ , \quad m_{\ell\ell} \notin [75, 105]\ GeV\ . \tag{9}$$

Tab. 4 summarizes our results in the channel $\ell^\pm\ell^\mp jj \not{E}_T$. In this table, we have shown the incremental effects on the cuts defined above on signal and background. As it can be seen from the table, the signal events are not much affected by the imposition of the cuts on the dijet and dilepton invariant masses, whereas we can substantially reduce the backgrounds arising from the $WWjj$ and $ZZjj$ channels.

We can also use the $\not{E}_T$ cut to further reduce the backgrounds. The $\not{E}_T$ cut is very useful, because in the SM, $\not{E}_T$ originates from neutrinos that come from the decay of W or Z, and hence it could be relatively soft, whereas in the LHT model, $\not{E}_T$ comes from a heavy particle, the T-odd photon (A_H), and hence it could be relatively hard. We have shown the $\not{E}_T$ distribution in Fig. 5, where one can see that the background can be reduced by using a harder $\not{E}_T$ cut. We have accordingly shown the results in Tab. 4 by using cuts $\not{E}_T > 200, 300, 400$ GeV

Table 4: *The σ numbers shown in the second row are with relevant K-factors included. The σ numbers in brackets (second row) are the cross section values, if we only include the QCD production mechanism without K-factors as considered in Choudhury et al. [5] as given in Eq. 5. The remaining rows indicate the number of events for the luminosity $\mathcal{L} = 100$ fb^{-1}. For the numbers given above, we have included both QCD and EW contributions.*

Parameter set $\Rightarrow$	$f = 1000$	$f = 1000$	$f = 700$	SM	SM	SM
Cuts $\Downarrow$	$\kappa = 0.6$	$\kappa = 1$	$\kappa = 1.5$	$t\bar{t}$	W^+W^-jj	$ZZjj$
Production σ (fb)	1039.1 (298)	157.4 (14.8)	412.3 (31.4)			
Preselection cuts	795.7	120.7	262.6	1.54×10^5	2.29×10^4	1520.6
$m_{jj} \notin [65, 105]$	755	120.1	261.7	1.26×10^5	1.88×10^4	1227.5
$m_{\ell\ell} \notin [75, 105]$	696.8	111.9	239.4	9.94×10^4	1.5×10^4	64.5
$\not{E}_T > 100$	623.8	108.8	234.5	2.5×10^4	4946.4	19.9
$\not{E}_T > 200$	441.2	100.5	220.3	2136.4	899.5	3.9
$\not{E}_T > 300$	237.3	87.5	200.1	396.1	239	1.3
$\not{E}_T > 400$	107.1	71.9	174.6	114.1	69.5	0.7
$\mathcal{S}$	7.2	4.9	11.2			

In addition, one can also use H_T (the total transverse energy) as the parameter to distinguish signal and backgrounds. The energy of the heavy particles produced (T-odd quarks for signal)

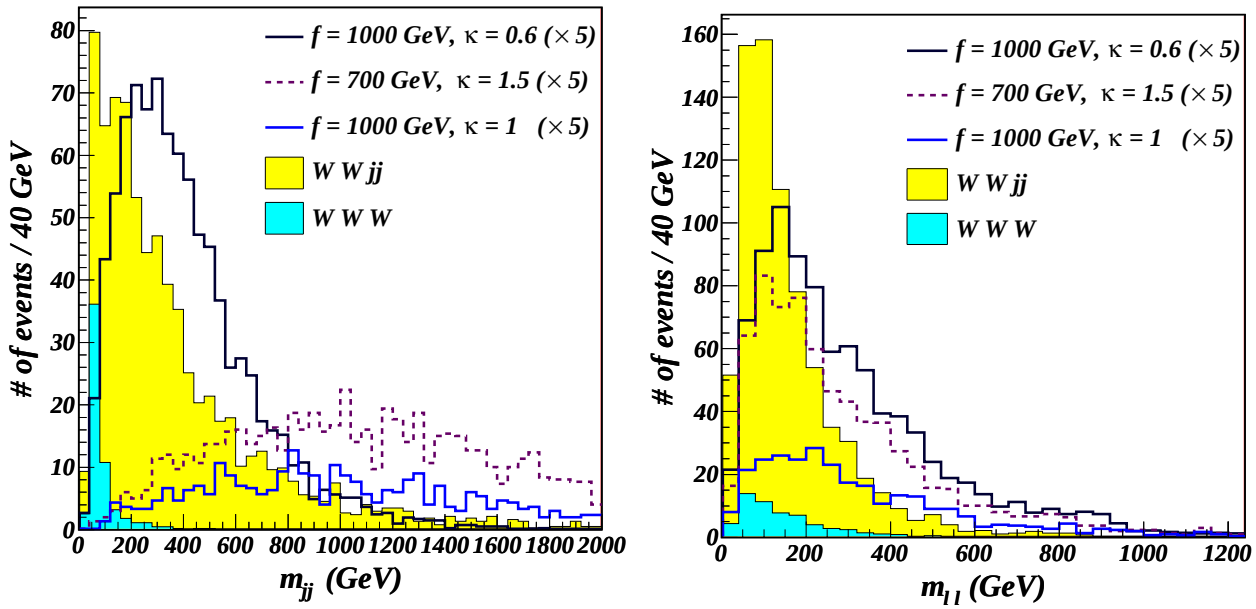

Figure 6: *$\not{E}_T$ distribution (left panel) and same-sign dilepton invariant mass ($m_{\ell^\pm \ell^p m}$) distribution (right panel) for signal ($\times 5$) and SM background in the channel $pp \to \ell^\pm \ell^\pm jj \not{E}_T$. In plotting these distributions we have assumed the LHC luminosity to be $\mathcal{L} = 100$ fb^{-1}.*

is essentially given to its various products, namely jets (j), leptons (ℓ) and $\not{E}_T$. Therefore one can define the total transverse energy (H_T) as :

$$H_T = \sum_{j,\ \ell,\ \not{E}_T} |\vec{p}_T|. \tag{10}$$

The H_T distribution peaks around the heavy particle mass, and a cut on H_T could be helpful in reducing the backgrounds. The H_T distribution is shown in Fig. 5. As the H_T distribution tends to peak around the heavy particle mass, it can also be used to estimate the T-odd quark masses.

C Same-sign dilepton signatures: $\ell^\pm \ell^\pm jj \not{E}_T$

This signature is generated by the production mechanism given in Eq. (7) and the decay chains given in Eqs. (4). The same sign dilepton signature has relatively less SM backgrounds and hence could be more useful to search for the T-odd quarks in pair production at LHC.
The possible backgrounds to our signal are:

- $pp \to W^\pm W^\mp W^\pm$, where one of the W-bosons decays into jets and the two same sign W-bosons decays leptonically. The production cross section for this process is 127 fb.
- $pp \to W^\pm W^\pm jj$ with both W-bosons decaying leptonically. The production cross section for this process is ~ 420 fb.

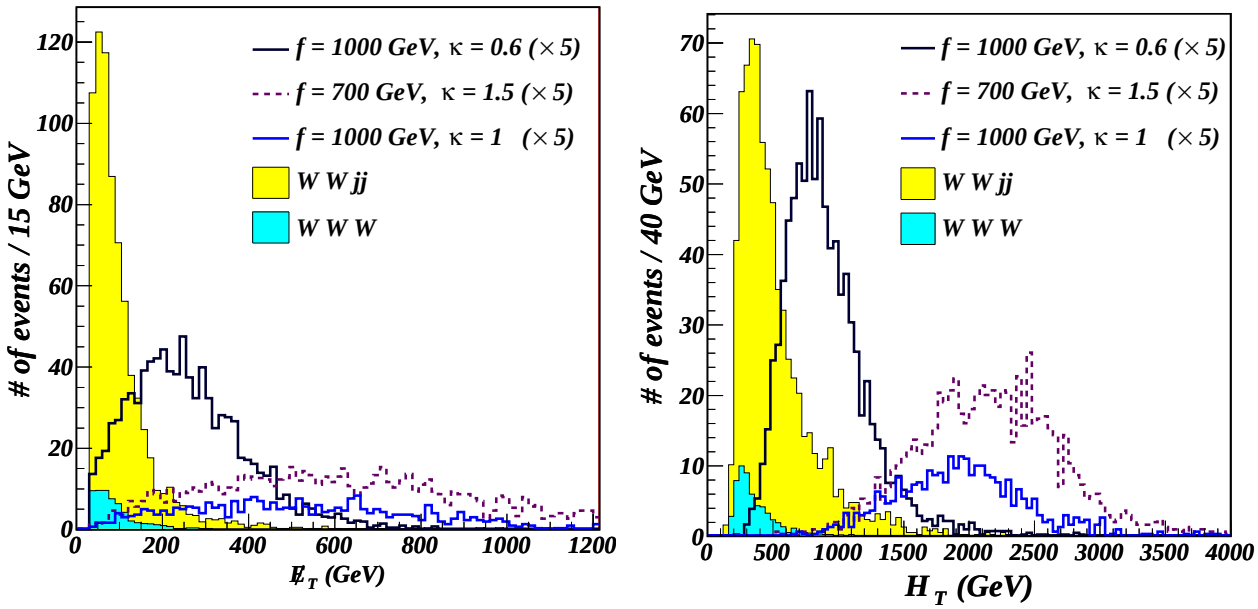

Figure 7: $\not{E}_T$ and H_T distribution (right panel) for signal ($\times 5$) and SM background in the channel $pp \to \ell^\pm\ell^\pm jj\ \not{E}_T$ for an LHC luminosity of $\mathcal{L} = 100\ fb^{-1}$.

The *pre-selection* cuts used are:

(a) exactly two light jets with $p_T^j > 30$ GeV and $|\eta| < 2.5$;

(b) exactly two leptons of same sign with $p_T^\ell > 15$ GeV and $|\eta| < 2.5$;

(c) a minimum missing energy threshold of $\not{E}_T > 30$ GeV.

In Fig. 6, we have shown the dijet invariant mass (m_{jj}) for light jets and the same-sign dilepton invariant mass ($m_{\ell^\pm\ell^\pm}$) distributions. We impose a cut on jet invariant mass of

$$|m_{jj} - M_W| > 20GeV\ . \tag{11}$$

This cut helps reducing the background coming from $W^\pm W^\mp W^\pm$. In Tab. 5, we have shown the effects of the pre-selection cuts and the cut on the dijet invariant mass on the signal and backgrounds.

As previously argued, in LHT models we expect to have hard $\not{E}_T$, and hence one can substantially reduce the SM backgrounds by using a hard $\not{E}_T$ cut. This is also evident from the $\not{E}_T$ distribution shown in Fig. 7. We have accordingly shown the number of expected events for $\not{E}_T > 200, 300, 400$ GeV.

Finally, for the signature $\ell^\pm\ell^\pm jj\ \not{E}_T$, we have shown the total transverse energy distribution (H_T). As previously argued, this distribution could be useful in having a estimate of the T-odd quark masses.

Table 5: Same-sign dilepton results in the channel $pp \to \ell^\pm\ell^\pm jj$ for $\mathcal{L} = 100$ fb^{-1}.

Parameter set $\Rightarrow$	$f = 1000$	$f = 700$	$f = 1000$	SM	SM
Cuts $\Downarrow$	$\kappa = 0.6$	$\kappa = 1.5$	$\kappa = 1$	$W^\pm W^\pm jj$	$W^\pm W^\pm W^\mp$
Production σ (fb)	235.1	240.7	80.1		
Pre-selection	180.5	140.9	58.5	747.2	59.1
$\lvert m_{jj} - M_W\rvert > 20$ GeV	173.9	140.6	58.5	651.2	20.3
$\not{E}_T > 100$	155.7	138.5	56.6	236.1	5.8
$\mathcal{S}$	9.1	8.2	3.5		
$\not{E}_T > 200$	108.4	129.4	51.6	57.8	0.9
$\not{E}_T > 300$	57.7	117.4	45.1	22.2	0.3
$\not{E}_T > 400$	24.9	103	37.5	9.6	0.1
$\mathcal{S}$	6.2	18.6	8.6		

VI Conclusions

In this paper, we have analyzed the signatures of the pair production of the first two generations of T-odd quarks in the context of the LHT model. We first showed that for a reasonable range of input parameters, these quarks can be produced in large numbers both at the low energy (10 TeV) run and the full 14 TeV run of the LHC. The T-odd quark masses depend only on κ and f. The branching fractions for the decays of these quarks crucially depend on κ: for large values ($\kappa > 0.462$), the main mode is in W_H plus a light quark and it can contain a lepton coming from the subsequent leptonic decay of the W.

In this work, we considered both same-sign and opposite-sign dilepton signatures: (a) opposite-sign dilepton pairs, $pp \to (\bar{Q}_H Q_H, Q_H Q'_H) \to (q\bar{q}, qq')W_H^\pm W_H^\mp \to jj\ell^\pm\ell^\mp \not{E}_T$, and (b) same-sign dilepton pairs, $pp \to Q_H Q'_H \to qq' W_H^\pm W_H^\pm \to jj\ell^\pm\ell^\pm \not{E}_T$. We used CalcHEP to generate the signal and further interfaced it with PYTHIA. For realistic estimates of signal and backgrounds, we used the fast ATLAS detector simulator ATLFAST. We also gave the possible K-factors for signal and background processes. As could be seen, the relevant K-factors can give substantial enhancements in the production rates of the first two generations of T-odd quarks at LHC.

To quantify our results, we have also shown the significance of the results for three sets of LHT model input points. As signal and background events after the cuts are smaller in number, we have to use the Poisson statistics to estimate the significance of the results. To quantify our results for the set of input parameters chosen, we use a significance estimator [29]

$$\mathcal{S} = \sqrt{2\left\{n_0\ ln\left(1 + \frac{s}{b}\right) - s\right\}},$$

where b is the expected number of background events and n_0 is the number of observed events. Accordingly, the signal is defined as $s = n_0 - b$. This estimator is based on a log-likelihood ratio and follows very closely the Poisson significance. We used the minimum set of pre-selection cuts as

defined in Sec. V for signal and background processes. We tried to analyze various distributions that could help in selecting secondary set of cuts to improve signal to background rates. We found that the hard cuts on $\not{E}_T$ could be useful in extracting the signal from the backgrounds. Accordingly, we showed the results of signal and background events for a $\not{E}_T$ cut of 100, 200, 300 and 400 GeV. The summary of the number of events after imposing various selection cuts were given in Tab. 4 (opposite-sign dilepton) and Tab. 5 (same-sign dileptons). As can be seen from the summary tables of the results, the signal to background ratio can be significantly improved in the case of same-sign dileptons and even further by using the H_T distribution. In case of opposite-sign dileptons, the $t\bar{t}$ backgrounds make the H_T-distribution peak at much larger values, and hence this distribution could be useful to improve signal to background, if the masses of T-odd quarks are much higher as compared to the SM top-quark. In the case of same-sign leptons, the backgrounds come from gauge bosons, and hence the H_T-distribution peaks at relatively lower values. Hence this distribution is much more useful to suppress backgrounds. At this point we would like to note, as is evident from Fig. 1, that the second leading decay channel of T-odd quarks is $Q_H \to Z_H q$. Although this is not the dominant decay chain, it can lead to some very interesting signatures [5]. This issue will be addressed in a future work [30]. In Tabs. 4 and 5, we have also given the expected significance ($\mathcal{S}$) of the results for three sets of LHT input parameters. The results indicate that the significance of the resuls in the signal (b), same-sign dileptons, provides a very interesting discovery potential, as the backgrounds in this channel are very low. This channel can also give a good estimate of the masses of T-odd quarks from the H_T-distribution. As can be seen from the results, one must optimise the secondary selection cuts to further improve the signal rates as compared to the backgrounds. This is beyond the scope of the present paper. To summarize, the pair production of T-odd quarks can probe a substantial (f, κ) region of the LHT model parameter space. For some reasonable values of κ using the same-sign dilepton channel described above, one can probe the symmetry breaking scale of the LHT model (f) up to the TeV range. We hope that this study will motivate the LHC collaborations to search for the first two generations of T-odd quarks at LHC.

Acknowledgements

We would like to thank Satyaki Bhattacharya, John Campbell, Debajyoti Choudhury, and Peter Skands for useful discussions/communications. We also like to thank A. Belyaev for providing us the original LANHEP files for the LHT model [8]. AD and MK are supported by the ANR project ANR-06-JCJC-0038-01 and the Theory-LHC-France initiative of the CNRS/IN2P3. The work of SRC was supported by Ramanna fellowship of Department of Science & Technology (DST), India.

References

[1] R. Barbieri and A. Strumia, arXiv:hep-ph/0007265.

[2] M. Schmaltz and D. Tucker-Smith, Ann. Rev. Nucl. Part. Sci. **55**, 229 (2005) [arXiv:hep-ph/0502182]; M. Perelstein, Prog. Part. Nucl. Phys. **58**, 247 (2007) [arXiv:hep-ph/0512128].

[3] C. Csaki, J. Hubisz, G. D. Kribs, P. Meade and J. Terning, Phys. Rev. D **68**, 035009 (2003) [arXiv:hep-ph/0303236]; T. Gregoire, D. Tucker-Smith and J. G. Wacker, Phys. Rev. D **69**, 115008 (2004) [arXiv:hep-ph/0305275]; R. Casalbuoni, A. Deandrea and M. Oertel, JHEP **0402**, 032 (2004) [arXiv:hep-ph/0311038]; Z. Han and W. Skiba, Phys. Rev. D **72**, 035005 (2005) [arXiv:hep-ph/0506206].

[4] H. C. Cheng and I. Low, JHEP **0309**, 051 (2003) [arXiv:hep-ph/0308199]; H. C. Cheng and I. Low, JHEP **0408**, 061 (2004) [arXiv:hep-ph/0405243]; H. C. Cheng, I. Low and L. T. Wang, Phys. Rev. D **74**, 055001 (2006) [arXiv:hep-ph/0510225].

[5] D. Choudhury and D. K. Ghosh, JHEP **0708**, 084 (2007) [arXiv:hep-ph/0612299].

[6] T. Goto, Y. Okada and Y. Yamamoto, Phys. Lett. B **670**, 378 (2009) [arXiv:0809.4753 [hep-ph]]; F. del Aguila, J. I. Illana and M. D. Jenkins, JHEP **0901**, 080 (2009) [arXiv:0811.2891 [hep-ph]]; M. Blanke, A. J. Buras, B. Duling, S. Recksiegel and C. Tarantino, arXiv:0906.5454 [hep-ph].

[7] A. Freitas and D. Wyler, JHEP **0611**, 061 (2006) [arXiv:hep-ph/0609103].

[8] A. Belyaev, C. R. Chen, K. Tobe and C. P. Yuan, Phys. Rev. D **74**, 115020 (2006) [arXiv:hep-ph/0609179].

[9] E. Richter-Was *et.al.* , *ATLFAST 2.2: A fast simulation package for ATLAS*, ATL-PHYS-98-131.

[10] I. Low, JHEP **0410**, 067 (2004) [arXiv:hep-ph/0409025].

[11] J. Hubisz and P. Meade, Phys. Rev. D **71**, 035016 (2005) [arXiv:hep-ph/0411264].

[12] J. Hubisz, P. Meade, A. Noble and M. Perelstein, JHEP **0601**, 135 (2006) [arXiv:hep-ph/0506042].

[13] P. Dey, S. K. Gupta and B. Mukhopadhyaya, Phys. Lett. B **674**, 188 (2009) [arXiv:0809.3893 [hep-ph]].

[14] M. Blanke, A. J. Buras, A. Poschenrieder, S. Recksiegel, C. Tarantino, S. Uhlig and A. Weiler, JHEP **0701**, 066 (2007) [arXiv:hep-ph/0610298]; M. Blanke, A. J. Buras, S. Recksiegel, C. Tarantino and S. Uhlig, JHEP **0706**, 082 (2007) [arXiv:0704.3329 [hep-ph]];

I. I. Bigi, M. Blanke, A. J. Buras and S. Recksiegel, JHEP **0907**, 097 (2009) [arXiv:0904.1545 [hep-ph]].

[15] S. R. Choudhury, A. S. Cornell, A. Deandrea, N. Gaur and A. Goyal, Phys. Rev. D **75**, 055011 (2007) [arXiv:hep-ph/0612327]; M. Blanke, A. J. Buras, B. Duling, A. Poschenrieder and C. Tarantino, JHEP **0705**, 013 (2007) [arXiv:hep-ph/0702136]; N. Gaur, AIP Conf. Proc. **981**, 357 (2008) [arXiv:0710.3998 [hep-ph]].

[16] H. C. Cheng, I. Low and L. T. Wang, Phys. Rev. D **74** (2006) 055001 [arXiv:hep-ph/0510225].

[17] A. Pukhov, arXiv:hep-ph/0412191.

[18] J. Pumplin, D. R. Stump, J. Huston, H. L. Lai, P. M. Nadolsky and W. K. Tung, JHEP **0207**, 012 (2002) [arXiv:hep-ph/0201195].

[19] J. R. Primack, D. Seckel and B. Sadoulet, Ann. Rev. Nucl. Part. Sci. **38**, 751 (1988).

[20] H. Burkhardt, *Status of LHC machine*, talk at Lepton-Photon 2009, Hamburg, Germany, August 2009.

[21] T. Sjostrand, S. Mrenna and P. Skands, JHEP **0605**, 026 (2006) [arXiv:hep-ph/0603175].

[22] J. Alwall *et al.*, arXiv:0712.3311 [hep-ph]; E. Boos *et al.*, arXiv:hep-ph/0109068 ; J. Alwall *et al.*, Comput. Phys. Commun. **176**, 300 (2007) [arXiv:hep-ph/0609017].

[23] F. Maltoni and T. Stelzer, JHEP **0302**, 027 (2003) [arXiv:hep-ph/0208156].

[24] J.M. Campbell, R.K. Ellis, `http://mcfm.fnal.gov/`.

[25] P. M. Nadolsky *et al.*, Phys. Rev. D **78**, 013004 (2008) [arXiv:0802.0007 [hep-ph]].

[26] M. Cacciari, S. Frixione, M. L. Mangano, P. Nason and G. Ridolfi, JHEP **0809**, 127 (2008) [arXiv:0804.2800 [hep-ph]].

[27] J. M. Campbell, R. Frederix, F. Maltoni and F. Tramontano, JHEP **0910**, 042 (2009) [arXiv:0907.3933 [hep-ph]].

[28] J. M. Campbell and R. K. Ellis, Phys. Rev. D **65**, 113007 (2002) [arXiv:hep-ph/0202176]; J. M. Campbell, R. K. Ellis and D. L. Rainwater, Phys. Rev. D **68**, 094021 (2003) [arXiv:hep-ph/0308195].

[29] G. L. Bayatian *et al.* [CMS Collaboration], J. Phys. G **34**, 995 (2007).

[30] G. Cacciapaglia, A. Deandrea, N. Gaur, M. Klasen, work in progress.